Inorg. Chem. **2009**, *48*, 3890−3895

Size- and Surface-Determined Transformations: From Ultrathin InOOH Nanowires to Uniform c-In_2O_3 Nanocubes and rh-In_2O_3 Nanowires

Xiangxing Xu and Xun Wang*

Department of Chemistry, Tsinghua University, Beijing, 100084, P. R. China

Received December 25, 2008

Ultrathin InOOH nanowires with a diameter of ∼2 nm and a length up to ∼200 nm have been synthesized by a hydrolysis reaction in a solution system. Their transformations to c-In_2O_3 nanocrystals and rh-In_2O_3 nanowires have been investigated. A dissolution−recrystallization (in solution) or size-related decomposition−recrystallization (in air) mechanism is indicated for the former transformation; the size- and surface-determined transformation is proposed for the latter. These results will help to understand and control the phase stability and transformation concerning the nanodimension and surface restrictions, especially for ultrathin nanowires.

Introduction

One of the main challenges in studying one-dimensional (1D) systems is the synthesis of ultrathin nanowires (diameter <5 nm).[1] In such a limited dimension, much attention has been focused on the novel features arising from the quantum effect, surface, mechanic, magnetic, and electronic properties.[2] However, the phase stability and transformation mechanisms are rarely studied, an understanding of which will shed light on the fundamental research and potential applications.

Polymorphous indium oxides (cubic-phased c-In_2O_3, corundum-type rh-In_2O_3, and Rh_2O_3-II-type In_2O_3), oxyhydroxide (InOOH), and hydroxide ($In(OH)_3$) make up a series of important wide-bandgap semiconductors.[3,4] They have been used in diverse areas including solar cells,[5] gas sensing,[6] biosensing,[7] electronics,[8] and catalysis.[9] A number of works observed that the annealing−dehydration of InOOH nanocrystals (diameter 7−50 nm) under temperatures of 300−600 °C and ambient pressure caused their transformation into rh-In_2O_3, while under similar conditions, $In(OH)_3$ nanocrystals were likely to transform into c-In_2O_3.[3c,h,6d,10] Two exceptional works reported that, by adopting different solvents, the $In(OH)_3$ and InOOH precursors evolved to c-In_2O_3 and rh-$In_2O_3$by annealing, selectively.[3e,11] But both of them gave

* To whom correspondence should be addressed. E-mail: wangxun@mail.tsinghua.edu.cn.

(1) (a) Tang, Z. Y.; Kotov, N. A.; Giersig, M. *Science* **2002**, *297*, 237–240. (b) Yu, H.; Li, J.; Loomis, R. A.; Gibbons, P. C.; Wang, L. W.; Buhro, W. E. *J. Am. Chem. Soc.* **2003**, *125*, 16168–16169. (c) Yu, H.; Li, J.; Loomis, R. A.; Wang, L. W.; Buhro, W. E. *Nat. Mater.* **2003**, *2*, 517–520. (d) Cademartiri, L.; Malakooti, R.; O'Brien, P. G.; Migliori, A.; Petrov, S.; Kherani, N. P.; Ozin, G. A. *Angew. Chem., Int. Ed.* **2008**, *47*, 3814–3817. (e) Lu, X. M.; Yavuz, M. S.; Tuan, H. Y.; Korgel, B. A.; Xia, Y. N. *J. Am. Chem. Soc.* **2008**, *130*, 8900–8901. (f) Huo, Z. Y.; Tsung, C. K.; Huang, W. Y.; Zhang, X. F.; Yang, P. D. *Nano Lett.* **2008**, *8*, 2041–2044.

(2) (a) Bezryadin, A.; Lau, C. N.; Tinkham, M. *Nature (London)* **2000**, *404*, 971–974. (b) Kan, S.; Mokari, T.; Rothenberg, E.; Banin, U. *Nat. Mater.* **2003**, *2*, 155–158. (c) Teng, X. W.; Han, W. Q.; Ku, W.; Hucker, M. *Angew. Chem., Int. Ed.* **2008**, *47*, 2055–2058. (d) Wang, C.; Hu, Y. J.; Lieber, C. M.; Sun, S. H. *J. Am. Chem. Soc.* **2008**, *130*, 8902–8903. (e) Xu, X. X.; Zhuang, J.; Wang, X. *J. Am. Chem. Soc.* **2008**, *130*, 12527–12535.

(3) (a) Avivi, S.; Mastai, Y.; Gedanken, A. *Chem. Mater.* **2000**, *12*, 1229–1233. (b) Liang, C. H.; Meng, G. W.; Lei, Y.; Phillipp, F.; Zhang, L. D. *Adv. Mater.* **2001**, *13*, 1330–1333. (c) Yu, D. B.; Yu, S. H.; Zhang, S. Y.; Zuo, J.; Wang, D. B.; Qian, Y. T. *Adv. Funct. Mater.* **2003**, *13*, 497–501. (d) Seo, W. S.; Jo, H. H.; Lee, K.; Park, J. T. *Adv. Mater.* **2003**, *15*, 795–797. (e) Epifani, M.; Siciliano, P.; Gurlo, A.; Barsan, N.; Weimar, U. *J. Am. Chem. Soc.* **2004**, *126*, 4078–4079. (f) Liu, Q. S.; Lu, W. G.; Ma, A. H.; Tang, J. K.; Lin, J.; Fang, J. Y. *J. Am. Chem. Soc.* **2005**, *127*, 5276–5277. (g) Zhu, H. L.; Yao, K. H.; Zhang, H.; Yang, D. R. *J. Phys. Chem. B* **2005**, *109*, 20676–20679. (h) Chen, C. L.; Chen, D. R.; Jiao, X. L.; Wang, C. Q. *Chem. Commun.* **2006**, 4632–4634. (i) Fang, Y. P.; Wen, X. G.; Yang, S. H. *Angew. Chem., Int. Ed.* **2006**, *45*, 4655–4658. (j) Narayanaswamy, A.; Xu, H. F.; Pradhan, N.; Kim, M.; Peng, X. G. *J. Am. Chem. Soc.* **2006**, *128*, 10310–10319. (k) Lee, C. H.; Kim, M.; Kim, T.; Kim, A.; Paek, J.; Lee, J. W.; Choi, S. Y.; Kim, K.; Park, J. B.; Lee, K. *J. Am. Chem. Soc.* **2006**, *128*, 9326–9327. (l) Shi, M. R.; Xu, F.; Yu, K.; Zhu, Z. Q.; Fang, J. H. *J. Phys. Chem. C* **2007**, *111*, 16267–16271. (m) Lu, W. G.; Liu, Q. S.; Sun, Z. Y.; He, J. B.; Ezeolu, C.; Fang, J. Y. *J. Am. Chem. Soc.* **2008**, *130*, 6983–6991. (n) Walsh, A.; Da Silva, J. L. F.; Wei, S. H.; Korber, C.; Klein, A.; Piper, L. F. J.; DeMasi, A.; Smith, K. E.; Panaccione, G.; Torelli, P.; Payne, D. J.; Bourlange, A.; Egdell, R. G. *Phys. Rev. Lett.* **2008**, *100*, 167402.

(4) (a) Shannon, R. D. *Solid State Commun.* **1966**, *4*, 629–630. (b) Reid, A. F.; Ringwood, A. E. *J. Geophys. Res.* **1969**, *74*, 3238–3252. (c) Atou, T.; Kusaba, K.; Fukuoka, K.; Kikuchi, M.; Syono, Y. *J. Solid State Chem.* **1990**, *89*, 378–384. (d) Gurlo, A.; Dzivenko, D.; Kroll, P.; Riedel, R. *Phys. Status Solidi* **2008**, *2*, 269–271. (e) Gurlo, A.; Kroll, P.; Riedel, R. *Chem.−Eur. J.* **2008**, *14*, 3306–3310. (f) Yusa, H.; Tsuchiya, T.; Tsuchiya, J.; Sata, N.; Ohishi, Y. *Phys. Rev. B* **2008**, *78*, 092107.

10.1021/ic802449w CCC: $40.75
Published on Web 03/27/2009

no close investigation on the nanocrystal size, morphology, or surface. To our knowledge, there is notably less data available on the phase stabilization and transformation mechanisms of nanocrystalline InOOH−c-In_2O_3−rh-In_2O_3 systems of ultrathin nanowires.

Herein, we report, for the first time, the controllable synthesis of InOOH nanocrystals (quantum dots, QDs) and ultrathin nanowires with diameters of ∼2 nm, showing a quantum confinement effect in the 0D→1D transformation. Unusually, the as-synthesized nanowires did not transform into rh-In_2O_3 in the subsequent annealing treatment in the air or in solution systems. Instead, they transformed into nanocrystals or uniform nanocubes of c-In_2O_3. By using a morphology-freezing strategy, that is, capping the InOOH nanowires with a silica shell, the thermal stability of InOOH was increased, and the following annealing at higher temperatures of 400−700 °C revealed the transformation to rh-In_2O_3 nanowires. These particular phenomena call for the reinterpretation of the phase-transformation mechanisms concerning unique nanostructures, for instance, ultrathin nanowires.

Experimental Section

In a typical synthesis of InOOH ultrathin nanowires, 0.06−0.1 g indium(III) chloride tetrahydrate ($InCl_3 \cdot 4H_2O$, AR) was dissolved in 5 mL of oleylamine (C18-content 80−90%, Acros). Then, 8 mL of ethanol was dropped in while ultrasonicating, forming a clear solution, which was transferred into a Teflon-lined stainless steel autoclave to react at 180 °C. The reaction time was controlled from 30 min to 12 h. The product was collected at the bottom, washed twice by adding 10 mL of ethanol, and centrifugation at 10 000 rpm for 10 min. The white product can be well redispersed in cyclohexane. In preparing c-In_2O_3 nanocubes, the reaction was carried out at 225 °C for 48 h.

Capping InOOH nanowires with SiO_2 involved the following: 4 mL of TX-100, 3 mL of n-hexanol, 1 mL of H_2O, and 0.1−0.6 mL of $NH_3 \cdot H_2O$ were mixed to form solution A. Then, 14 mL of cyclohexane containing 63 mg of InOOH nanowires and 2 mL of cyclohexane solution containing 0.07−0.6 mL of tetraethyl orthosilicate (TEOS) were sequentially added to solution A while it was kept stirring for 12 h. The coated InOOH nanowires were separated by centrifugation. The overall experimental routes investigated in this paper are illustrated in Scheme SP-1 (in the Supporting Information).

The phase purity of the products was verified by powder X-ray diffraction (XRD) on a Bruker D8 advance X-ray diffractometer using Cu Kα radiation ($\lambda = 1.5418$Å). The size and morphology of the nanocrystals were measured using a JEOL JEM-1200EX transmission electron microscope (TEM) at 120 kV, a Tecnai G2 F20 S-Twin high-resolution transmission electron microscope (HRTEM) at 200 kV, and JEOL JSM-6700F and JSM-7401 scanning electron microscopes (SEM). UV−vis absorption spectra were measured using a Hitachi U-3010 spectrophotometer. Photoluminescence (PL) spectra were recorded with a Hitachi F-4500 fluorescence spectrophotometer. FT-IR spectroscopy was performed on a Nicolet 560 spectrograph. Thermogravimetric analysis (TGA) measurements were carried out on 2050 TGA V5.3C instruments.

Results and Discussion

The synthesis of InOOH nanowires is based on the hydrolysis reaction of In^{3+} in an oleylamine and ethanol mixture solution at 180 °C:

$$In^{3+} + 3H_2O \rightarrow In(OH)_3 + 3H^+ \quad (1)$$

$$In(OH)_3 \rightarrow InOOH + H_2O \quad (2)$$

At 180 °C, InOOH nanocrystals or ultrathin nanowires were synthesized, while neither InOOH nor $In(OH)_3$ was obtained at 170 °C or lower reaction temperatures. It indicates that reaction 2 follows reaction 1 immediately, along with InOOH nucleation and growth. InOOH nanocrystals of 1−3 nm were synthesized at a short reaction time of 10−30 min (Figure 1A,B). Short InOOH nanowires were obtained when the reaction time was prolonged to 1 h (Figure 1C). Raising the In^{3+} concentration from 0.015 to 0.025 M also helped increase the final (10 h) nanowire length, while the diameter of ∼2 nm remained almost unchanged (Figure 1E−G). The XRD spectrum indicated that the product is the orthorhombic InOOH (JCPDS card No. 71-2283). A "V"-shaped structure was generally observed in those InOOH nanowires. HRTEM shows that both sides of one "V" structure share the (101) plane and grow in the [001] direction (Figure 1D). The growth direction of the InOOH nanowires is further verified by XRD; the (002) peak is relatively stronger (Figure 2E, Figure SP-3 in the Supporting Information). The oriented attachment mechanism is suggested for the InOOH nanowire growth; that is, most of the dot-shaped InOOH nanocrystals attach and connect in the [001] direction, forming InOOH nanowires. When two dots/nanowires attach with the (101) plane, a "V"-shaped structure is formed. The oleylamine serves not only as a solvent but also, more importantly, as a coordination template.[1e,f] The N−H modes of 1637 and 1635 cm^{-1} in the FT-IR spectrum (Figure 3) indicate that both the InOOH nanowires and c-In_2O_3 nanocubes are capped with oleylamine. The 2800−3000 cm^{-1} modes in the InOOH

(5) (a) Katoh, R.; Furube, A.; Yoshihara, T.; Hara, K.; Fujihashi, G.; Takano, S.; Murata, S.; Arakawa, H.; Tachiya, M. *J. Phys. Chem. B* **2004**, *108*, 4818–4822. (b) Hara, K.; Sayama, K.; Arakawa, H. *Sol. Energy Mater. Sol. Cells* **2000**, *62*, 441–447.
(6) (a) Gurlo, A.; Barsan, N.; Weimar, U.; Ivanovskaya, M.; Taurino, A.; Siciliano, P. *Chem. Mater.* **2003**, *15*, 4377–4383. (b) Pinna, N.; Neri, G.; Antonietti, M.; Niederberger, M. *Angew. Chem., Int. Ed.* **2004**, *43*, 4345–4349. (c) Zhang, D. H.; Liu, Z. Q.; Li, C.; Tang, T.; Liu, X. L.; Han, S.; Lei, B.; Zhou, C. W. *Nano Lett.* **2004**, *4*, 1919–1924. (d) Zhuang, Z. B.; Peng, Q.; Liu, J. F.; Wang, X.; Li, Y. D. *Inorg. Chem.* **2007**, *46*, 5179–5187.
(7) (a) Li, C.; Curreli, M.; Lin, H.; Lei, B.; Ishikawa, F. N.; Datar, R.; Cote, R. J.; Thompson, M. E.; Zhou, C. W. *J. Am. Chem. Soc.* **2005**, *127*, 12484–12485. (b) Curreli, M.; Li, C.; Sun, Y. H.; Lei, B.; Gundersen, M. A.; Thompson, M. E.; Zhou, C. W. *J. Am. Chem. Soc.* **2005**, *127*, 6922–6923.
(8) (a) Thomas, G. *Nature (London)* **1997**, *389*, 907–908. (b) Wager, J. F. *Science* **2003**, *300*, 1245–1246. (c) Li, C.; Zhang, D. H.; Han, S.; Liu, X. L.; Tang, T.; Zhou, C. W. *Adv. Mater.* **2003**, *15*, 143–146. (d) Nguyen, P.; Ng, H. T.; Yamada, T.; Smith, M. K.; Li, J.; Han, J.; Meyyappan, M. *Nano Lett.* **2004**, *4*, 651–657.
(9) Li, Z. H.; Xie, Z. P.; Zhang, Y. F.; Wu, L.; Wang, X. X.; Fu, X. Z. *J. Phys. Chem. C* **2007**, *111*, 18348–18352.
(10) (a) Tang, Q.; Zhou, W. J.; Zhang, W.; Ou, S. M.; Jiang, K.; Yu, W. C.; Qian, Y. T. *Cryst. Growth Des.* **2005**, *5*, 147–150. (b) Xu, J. Q.; Chen, Y. P.; Pan, Q. Y.; Xiang, Q.; Cheng, Z. X.; Dong, X. W. *Nanotechnology* **2007**, *18*, 115615. (c) Zhu, H.; Wang, X. L.; Yang, F.; Yang, X. R. *Cryst. Growth Des.* **2008**, *8*, 950–956.
(11) Chu, D. W.; Zeng, Y. P.; Jiang, D. L.; Xu, J. Q. *Nanotechnology* **2007**, *18*, 435605.

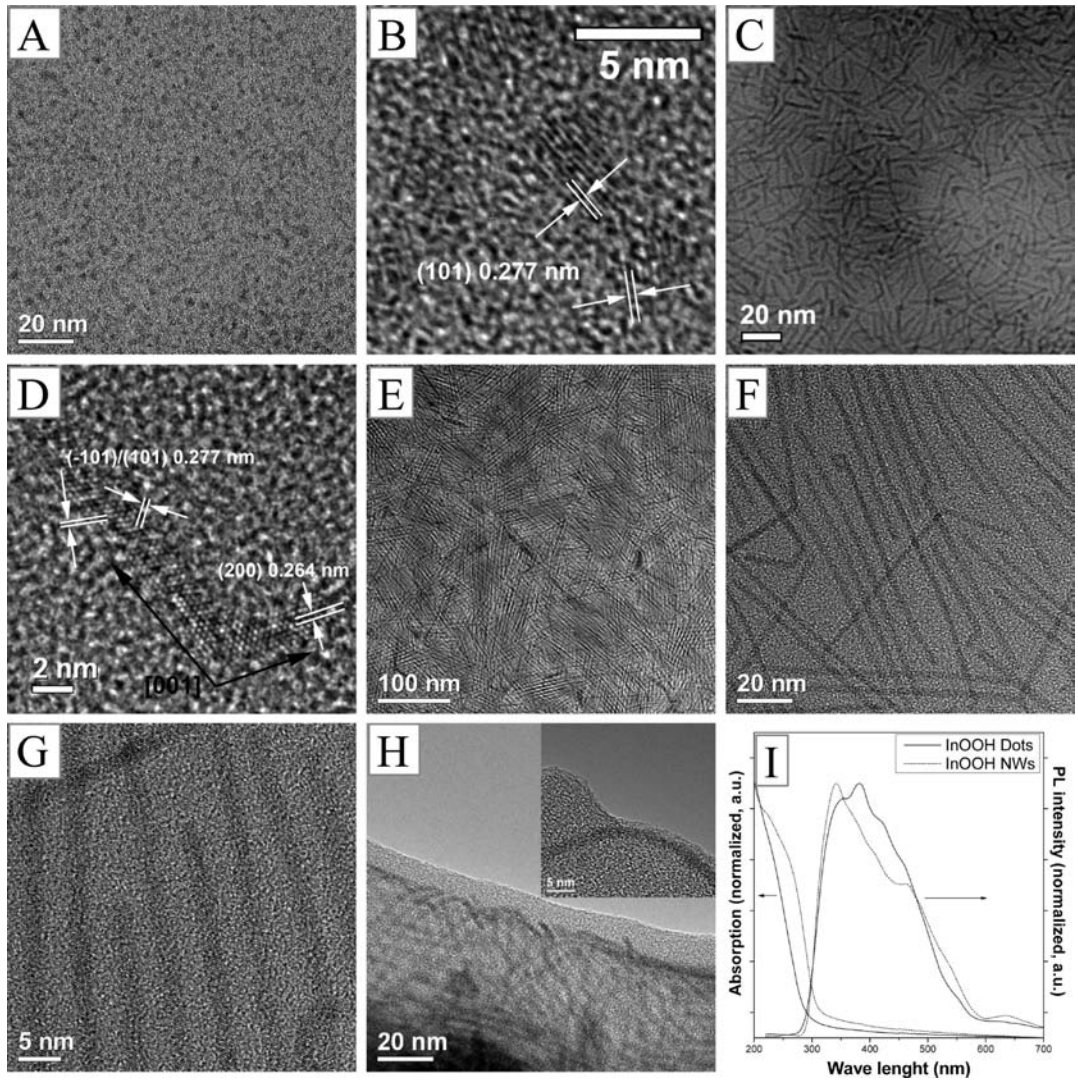

Figure 1. TEM/HRTEM images of InOOH nanocrystals and nanowires and their optical properties. (A, B) Dot-shaped InOOH nanocrystals. (C, D) Short InOOH nanowires. (E−G) Ultrathin InOOH nanowires with lengths up to ∼200 nm. (H) The ultrathin InOOH nanowires show great flexibility. (I) The absorption and photoluminescent spectra of InOOH dots and ultrathin nanowires.

sample are assigned to the CH_2 and CH_3 symmetric and asymmetric stretching vibrations, and the 1465 cm^{-1} peak is the CH_2 bending vibration mode. The broad absorption peak at 3438−3470 cm^{-1} may correspond to the −OH group of H_2O, suggesting the existence of water absorbed on the surface of both InOOH nanowires and c-In_2O_3 nanocubes. The peaks at 400−500 cm^{-1} are the In−O feature modes. Although the crystalline InOOH nanowires are intrinsically straight, they show surprising flexibility, looping or bending at the pore edge of the carbon film (Figure 1H).

The absorption spectrum was measured by dip-coating−drying a quartz slide. The absorption spectra indicate the quantum confinement effects of the InOOH 0D→1D system: the bandgaps of InOOH nanocrystals and nanowires determined by the absorption spectra differential maxima are 255 (4.86 eV) and 289 nm (4.32 eV), respectively (Figure SP-2 in the Supporting Information), or they are 286 (4.32 eV) and 315 nm (3.94 eV) if measured from the onset of the adsorption edge. The PL spectra of InOOH QDs and nanowires are almost overlapped within 280−580 nm, except that the nanowire PL spectrum has an apparent shoulder at 460 nm. The PL spectra are supposed to be coeffected results from the quantum confinement effect, surface effect, and defect states.[2e]

At a higher temperature of 225 °C for 48 h, uniform c-In_2O_3 nanocubes of a side length of ∼200 nm were incubated (Figure 4, and Figure SP-1D in the Supporting Information). Although the calcination−dehydration of In-$(OH)_3$ yielded c-In_2O_3, uniform $In(OH)_3$ nanocubes were hardly obtained. More over, the annealing of $In(OH)_3$ cubes may suffer from structure collapse and surface defects due to the dehydration.[12] Therefore, starting from the ultrathin InOOH nanowires was proved to be a new and effective alternation. Shortening the reaction time to less than 2 h shows that, in the primary stage, the InOOH nanowires coexist with some particles (Figure 4A). Those particles are c-In_2O_3 precubes, indicated by XRD (Figure SP-3 in the Supporting Information). Figure 4B shows the HRTEM measurement of one c-In_2O_3 precube and its FFT pattern. With the elongation of reaction time, the portion of InOOH

(12) Du, J.; Yang, M.; Cha, S. N.; Rhen, D.; Kang, M.; Kang, D. J. *Cryst. Growth Des.* **2008**, *8*, 2312–2317.

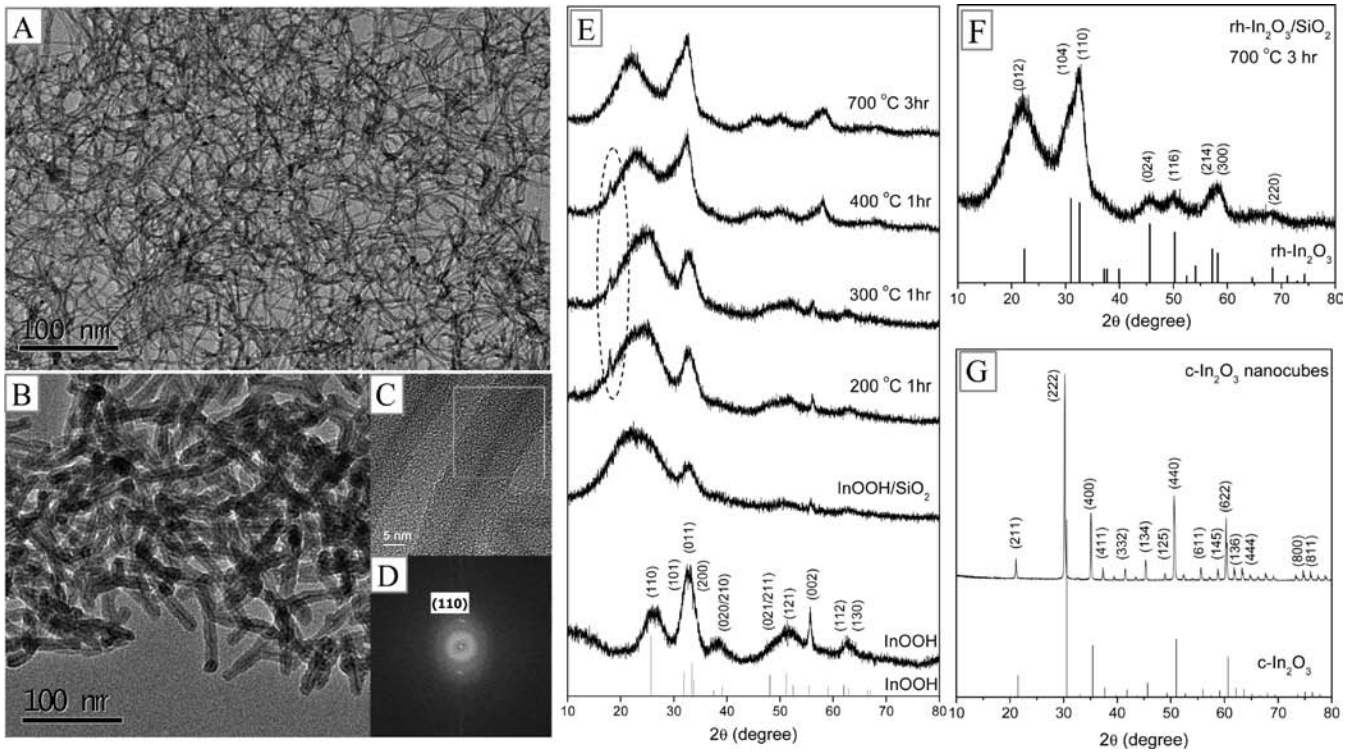

Figure 2. HRTEM images of (A) $InOOH/SiO_2$ with an outer diameter of 3−4 nm. (B, C) rh-In_2O_3/SiO_2 nanowires by annealing $InOOH/SiO_2$ (outer diameter 13−14 nm) at 700 °C for 3 h. (D) The FFT pattern in the marked square in C indicates the rh-In_2O_3 structure. (E) XRD patterns of InOOH ultrathin nanowires, $InOOH/SiO_2$, and its annealing samples, (F) rh-In_2O_3/SiO_2, rh-In_2O_3 JCPDS No. 22-0336, and (G) c-In_2O_3 nanocubes, c-In_2O_3 JCPDS No. 98-4595.

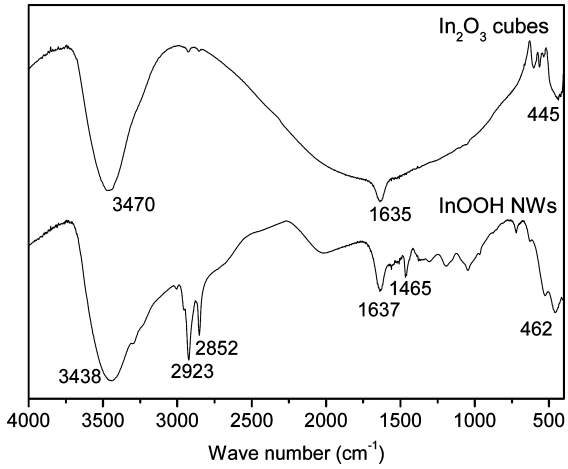

Figure 3. FT-IR spectra of the ultrathin InOOH nanowires and uniform c-In_2O_3 nanocubes.

nanowires decreases and the c-In_2O_3 precubes increases both in number and size. This process is described as a dissolution−recrystallization mechanism: under certain conditions, the InOOH ultrathin nanowires decompose and dissolve into the solution; with the InOOH nanowires' consumption, the c-In_2O_3 nuclei or monomer species originate. Those c-In_2O_3 nuclei self-assemble in an oriented fashion to each other, forming the coarse-surfaced but single-crystallized c-In_2O_3 precubes. The Ostwald ripening mechanism brings about the size distribution narrowing. At the same time, the ripened c-In_2O_3 nanocrystal surface converges to specific crystal facets in reducing the surface energy, forming truncated nanocubes. The cube facets of {200} and the truncated facets of {420} were verified by HRTEM. From SEM, it can be seen that the nanocube octal corners are truncated with {111} facets (see Figure 4G and Figure SP-4 in the Supporting Information). During the dry process of cyclohexane containing c-In_2O_3 nanocubes, the nanocubes can be ordered packed (Figure 4E,H and Figure SP-1D in the Supporting Information). The UV absorption maximum of the c-In_2O_3 nanocube sample is around 290 nm. The PL peak at 396 nm (Figure 4I) is assigned to the oxygen deficiency.

Annealing InOOH ultrathin nanowires at 200 °C for 2 h under ambient pressure in the air gives no change in either the morphology or the phase structure. At 250 °C for 2 h, the structure of InOOH nanowires is broken, while the phase is still pure InOOH measured by XRD. At 300 °C for 30 min, the InOOH ultrathin nanowires transformed into c-In_2O_3 nanocrystals (10−100 nm, Figure SP-1B, Supporting Information) completely. TGA (Figure 5) measurement shows that, below 300 °C, the weight loss can be assigned mainly to the capping oleylamine; at higher temperatures of >300 °C, the InOOH to c-In_2O_3 transformation contributes to the weight loss, additionally. The measured weight loss from 350 to 450 °C is 11.1% (theoretic InOOH→c-In_2O_3 value 6.1%). Therefore, the transformation mechanism is concluded as follows: in the beginning, the InOOH nanowire structure is deformed; then, the decomposition−dehydration takes place, which generates c-In_2O_3 nuclei. Those c-In_2O_3 nuclei aggregate and grow into c-In_2O_3 nanocrystals.

Realizing that, in both solution and air annealing that leads to the InOOH−c-In_2O_3 transformation, the dissolution/decomposition of InOOH ultrathin nanowires is the critical

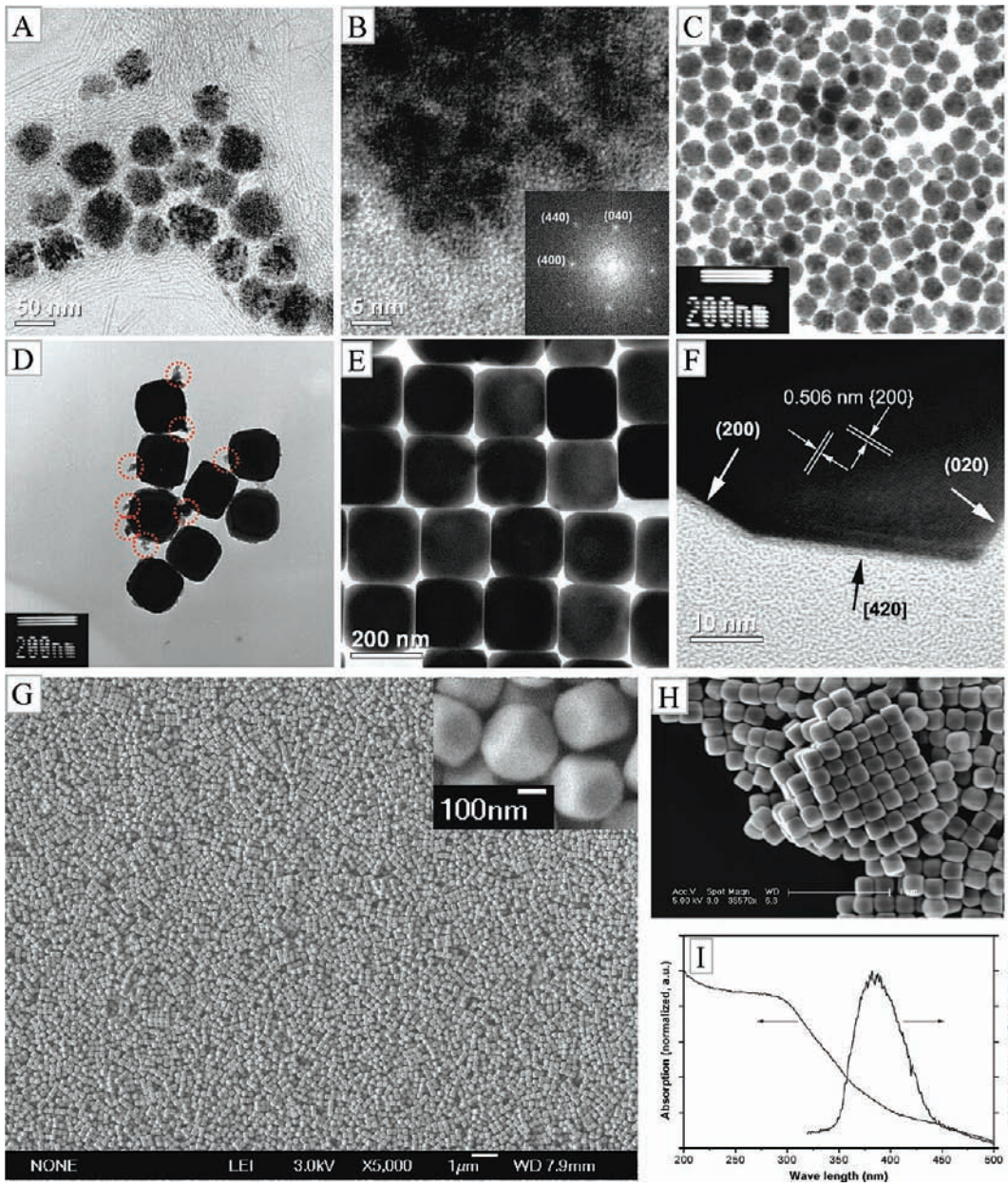

Figure 4. TEM/HRTEM/SEM images of ultrathin InOOH nanowires to uniform c-In_2O_3 nanocubes. (A) In the primary stage, c-In_2O_3 prenanocubes originate/coexist with InOOH nanowires. (B) HRTEM of one c-In_2O_3 prenanocube and its FFT image, indicating the single crystalline pattern. (C) Pure c-In_2O_3 prenanocubes. (D) Ostwald ripening process of the c-In_2O_3 nanocubes. Circled: attaching and dissolving of the smaller c-In_2O_3 nanocrystals to bigger ones. (E) HRTEM image of ripened uniform c-In_2O_3 nanocubes and (F) the cubic crystal structure. (G) SEM image of uniform c-In_2O_3 nanocubes and (H) the self-assembled structures. (I) The absorption and photoluminescent spectrum of the c-In_2O_3 nanocubes.

step toward the formation of c-In_2O_3 nanocrystals, and a "wrap−bake" strategy[13] was designed to prevent this process, that is, capping the InOOH nanowire surface and following with heat treatment. Silica is chosen as the capping shell because of its chemical inertness and amiability to covering various surfaces and the feasibility of preparing it under base and room temperature conditions, which will not destroy the InOOH ultrathin nanowires. The thickness of the silica shell can be controlled by the concentration and hydrolysis process of TEOS (Figure 2A−D). The InOOH/SiO_2 core/shell nanowires were then annealed under ambient pressure in the air with temperatures ranging from 200 to 700 °C. XRD spectra indicate that annealing at 200 or 300 °C for 1 h brings no obvious phase change of InOOH (225 °C annealing in solution has the same result); that is, the silica-protected InOOH ultrathin nanowires are more thermally stable than "naked" ones. When InOOH/SiO_2 nanowires were annealed at 400 °C or higher to 700 °C for more than 1 h, they transformed into rh-In_2O_3/SiO_2(Figure 2E,F).

From these results, it is obvious that the size, surface, and nanostructure do play crucial roles in the nanocrystalline InOOH−c-In_2O_3−rh-In_2O_3 transfromations. Yet, how the silica capping can induce the InOOH to rh-In_2O_3 transformation is still subject to speculation: does the core/shell structure generate high H_2O (from dehydration) pressure that triggers the transformation at elevated temperatures, or does the core/

(13) Piao, Y.; Kim, J.; Bin Na, H.; Kim, D.; Baek, J. S.; Ko, M. K.; Lee, J. H.; Shokouhimehr, M.; Hyeon, T. *Nat. Mater.* **2008**, *7*, 242–247.

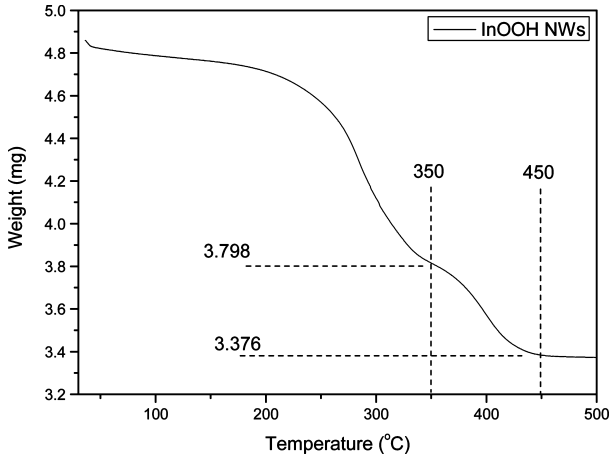

Figure 5. TGA curve of the ultrathin InOOH nanowires (temperature increasing rate: 10 °C/min).

shell interface reconstruction strain lead to the rh-In_2O_3 transformation? An unidentified XRD peak appears at 18.0° (2θ) in 200, 300, and 400 °C annealed samples (Figure 2E), which possibly suggests a new phase from InOOH to rh-In_2O_3.

Conclusions

In summary, we report the facile synthesis of ultrathin InOOH nanowires with a diameter of ~2 nm and a length up to ~200 nm. Its transformation to uniform c-In_2O_3 nanocubes and rh-In_2O_3 nanowires has been investigated. The dissolution− or decomposition−recrystallization mechanism is responsible for the InOOH−c-In_2O_3 transformation. The small diameter of the InOOH nanowires is demonstrated to be the critical factor that prevents its direct transformation into rh-In_2O_3 nanowires through annealing. By capping InOOH nanowires with a silica shell, this transformation is successfully revealed. We believe that these results will help to understand and control the phase stability and transformation concerning the size and surface restriction in the low dimensional nano world.

Acknowledgment. This work was supported by NSFC (20725102, 50772056), the Foundation for the Author of National Excellent Doctoral Dissertation of P. R. China, the Program for New Century Excellent Talents of the Chinese Ministry of Education, the Fok Ying Tung Education Foundation (111012), and the State Key Project of Fundamental Research for Nanoscience and Nanotechnology (2006CB932301).

Supporting Information Available: Schematic illustration and TEM/SEM images of ultrathin InOOH nanowires and their transformation to c-In_2O_3 nanocrystals by annealing in the air and in solution. Differential of the absorption spectra of the InOOH QDs and ultrathin nanowires. TEM/XRD measurement of the samples in the c-In_2O_3 precube formation stage. Crystal structure of the truncated c-In_2O_3 nanocubes. This material is available free of charge via the Internet at http://pubs.acs.org.

IC802449W